Corrosion behaviour of rolled A356 matrix composite reinforced with ceramic particles

S. O. R. Sheykholeslami[1], R. Taherzadeh Mousavian[1,*], D. Brabazon[2]

1: Faculty of Materials Engineering, Sahand University of Technology, Tabriz, Iran
2: Advanced Processing Technology Research Centre, School of Mechanical & Manufacturing Engineering, Dublin City University, Dublin 9, Ireland

Email: r_taherzadeh@sut.ac.ir
Tel: +98 919 959 1160, Fax: +98 21 44412039

Abstract

Hybrid ceramic particulate reinforced A356 aluminium composites were prepared via the semi-solid stir casting process followed by hot rolling. Fine micron-sized SiC powders and large micron-sized Al_2O_3 particles were used. The particles were coated in order to increase the ceramic incorporation and bonding with the metal. The corrosion behaviour of the composites was investigated using potentiodynamic polarization measurements. The results indicated that nickel coating and particles agglomeration of the fine SiC particles led to an increase in the corrosion current density in Tafel polarization curves. It was concluded that the composite manufacturing route employed reduced the corrosion resistance of rolled A356 alloy.

Keywords: Aluminium matrix composite; Corrosion; Polarization; Casting; Rolling.

1. Introduction

Al–Si based alloys are used for the production of automotive engine and other vehicular transport components where light weight, high-modulus, and high-strength are required [1-11]. Although specialty high-strength aluminium alloys have been developed, the addition of alloying elements and microstructural modification, can be costly, contain toxic elements, and often result in properties, which provide only a slight increase in mechanical properties. The demand for cost-effective lightweight, high-modulus, and high-strength materials has therefore led to the development of aluminium metal matrix composites (AMMCs) [12-19].

Stir casting in the semi-solid state is the most common route for producing of AMMCs [20-31] in which low wettability of the reinforcing phase is challenging. One of the methods for improving reinforcement wetting is to reduce the surface energy of the solid-liquid interface by a metallic coating of reinforcements [21, 32-34]. In 1981, Rohatgi [35] suggested using a metallic layer (copper coating) on ceramic particles for increasing their wettability by molten aluminium. Later, Rajan et al. [36] reported in more detail the role of the coating on reinforcement particles on the wettability and interface characteristics of aluminium metal matrix composites.

Corrosion resistance is an important material characteristic that should be taken into account in materials selection for industrial applications. In the case of AMMCs, it has been reported that they have lower corrosion resistance compared to the base alloys due to the destruction of predictive oxide film caused by the presence of ceramic particles [37]. Galvanic coupling between the matrix and the reinforcing phase also occurs when the reinforcing phase is not inert. It has been reported in the literature [38-40] that in contrast with most ceramic particles, some of the intermetallic phases show galvanic corrosion with the matrix. The intermetallic phases might be formed between the elements of an alloy or might be formed as a result of a reaction between the metallic coating layers such as copper and nickel with the matrix melt. In addition, it has been reported that crevice and pitting corrosion could occur at the interface of ceramic particles with the matrix [41]. The corrosion occurrence in the α-phase adjacent to intermetallic regions and also pitting corrosion in the dendrite cores were also shown to occur in AMMCs [42]. Singh et al. [41] reported that agglomeration of SiC powders caused a decrease in the corrosion resistance of AMMCs. El-Khair et al.[43] reported that Ni coating layer on the reinforcing phase caused a higher corrosion protection due to its higher electrode potential.

In this study, nickel and copper-coated hybrid ceramic particles with different particle sizes were incorporated into a semi-solid melt of A356 aluminium alloy. The composites were then hot rolled and their corrosion properties were evaluated using potentiodynamic polarization measurements in 3.5wt.% NaCl solution to identify the factors affecting their corrosion resistance.

2. Material and methods

The a356 aluminium ingot was used as a matrix material. Table 1 shows the chemical composition of the ingot as obtained using an M5000 optical emission spectrometer, Focused Photonics Inc., China.

Table 1
The chemical composition (in wt. %) of A356 aluminium alloy used in this study.

Al	Si	Mg	Fe	Cu	Mn	Zn	Ni	Ti
Bal.	7.2	0.33	0.11	0.01	0.02	0.02	0.03	0.01

SiC particles with an average particle size of 15 μm and 99.7% purity and coarse alumina particles with an average particle size of 170 μm and 99.4% purity which were supplied from Shanghai Dinghan Chemical Co., Ltd. China, were used as reinforcement. The alumina and SiC particles were coated with Cu and Ni layers using the electroless deposition (ED) method. The preparation procedure of the ED used for the production of the metallic coating on ceramic particles has been reported in previous studies [21, 33]. Tables 2 and 3 show the utilized ED

parameters including the chemicals, their concentrations, pH, temperature, and stirring speed.

Table 2

The composition of bath used for electroless deposition of the Ni-P coating onto the ceramic particles and coating parameters used.

Role in bath	Composition		Concentration
Main salt	Nickel sulfate	$NiSO_4.6H_2O$	25 g/l
Reducing agent	Sodium hypophosphite	$NaH_2PO_2.H_2O$	27.6 g/l
Complexing agent	Tri-sodium citrate	$C_6H_5Na_3O_7.2H_2O$	46 g/l
Buffering agent	Acid boric	H_3BO_3	26 g/l
pH adjuster	Sodium hydroxide	NaOH	To adjust pH
Ceramic powder (SiC/Al_2O_3)			22.5 g/1000ml
Operation	Magnetic stirring Temperature pH		400 rpm 50 ºC 8

Table 3

The composition of bath used for electroless deposition of the copper coating onto the ceramic particles and coating parameters used.

Role in bath	Composition		Concentration
Main salt	Copper sulphate	$CuSO_4·5H2O$	18 g/l
Reducing agent	Formaldehyde	HCHO	20 g/l
Complexing agent	Potassium sodium tartrate	$C_4H_4O_6KNa·4H_2O$	48 g/l
pH adjuster	Sodium hydroxide	NaOH	To adjust pH
Ceramic powders (SiC/Al_2O_3)			15 g / 660 ml
Operation	Magnetic stirring Temperature pH		400 rpm 60 ºC 10

Nine samples were fabricated in this study for comparing the effects ceramic addition to the matrix, ceramic type, and hybrid ceramic particle size distribution

on the corrosion properties of the composites. Table 4 summarizes the characteristics of the nine samples prepared in this study as well as the weight of the ceramic powders before and after ED.

Table 4

Characteristics of the samples fabricated in this study as well as the weight of the powders before and after ED process.

Samples ($ceramic\ particle_{coated\ metal}$)	Characteristics	Powder weight before coating	Powder weight after coating
$S_{1\ (unreinforced)}$	A356 as matrix	-	-
$S_{2\ (SiC_{Ni})}$	A356 as matrix, 3 wt. % SiC as reinforcement	15g SiC	17.8g (15g SiC+ 2.8g Ni)
$S_{3\ (Al_2O_{3_{Ni}})}$	A356 as matrix, 3 wt. % alumina as reinforcement	15g alumina	18.3g (15g alumina+ 3.3g Ni)
$S_{4\ (Al_2O_{3_{Ni}}-SiC_{Ni})}$	A356 as matrix, 1.5 wt. % alumina and 1.5 wt. % SiC as reinforcement	15g (7.5g alumina + 7.5g SiC)	18.05g (7.5g alumina + 7.5g SiC + 3.02g Ni)
$S_{5\ (SiC_{Cu})}$	A356 as matrix, 3 wt. % SiC as reinforcement	15g SiC	18.43g (15g SiC+ 3.43g Cu)
$S_{6\ (Al_2O_{3_{Cu}})}$	A356 as matrix, 3 wt. % alumina as reinforcement	15g alumina	17.60g (15g alumina+ 2.6g Cu)
$S_{7\ (Al_2O_{3_{Cu}}-SiC_{Cu})}$	A356 as matrix, 1.5 wt. % alumina and 1.5 wt. % SiC as reinforcement	15g (7.5g alumina + 7.5g SiC)	18.05g (7.5g alumina + 7.5g SiC + 3.05g Cu)
$S_{8\ (Al_2O_{3_{Cu}}-SiC_{Ni})}$	A356 as matrix, 1.5 wt. % alumina and 1.5 wt. % SiC as reinforcement	15g (7.5g alumina + 7.5g SiC)	17.7g (7.5g alumina + 7.5g SiC + 1.3g Cu+1.4g Ni)
$S_{9\ (Al_2O_{3_{Ni}}-SiC_{Cu})}$	A356 as matrix, 1.5 wt. % alumina and 1.5 wt. % SiC as reinforcement	15g (7.5g alumina + 7.5g SiC)	18.36g (7.5g alumina + 7.5g SiC + 1.715g Cu+1.65g Ni)

The composites were produced by bottom-pouring stir casting system under argon atmosphere. For this purpose, one gram of reinforcement powder for the composite samples was encapsulated carefully in an aluminum foil packet before

the stir casting process in order to fabricate a composite with 3 wt. % ceramic powders as reinforcement. The coated powders were wrapped by hand in aluminum foil with a precaution taken not to abrade the coated ceramics. These packets were pre-heated at 350 °C for 2 h in order to remove the moisture and impurities from the powders. The A356 alloy (500 g) was heated to 640 °C using a resistance furnace in order to have uniform melt condition. The melt was cooled to 600 °C corresponding to a 0.3 solid fraction. As-cast samples of 70 mm length, 15 mm width, and 6 mm thickness were then machined from solidified composites before rolling. The machined composite samples were held for 30 min at 500 °C in a preheated furnace and then were hot-rolled with four passes and with a thickness reduction of 1 mm per pass (67% reduction) and followed by one cold rolling pass at room temperature with a thickness reduction of 20%, resulting in a final sheet thickness of 1.6 mm. The rolling process was carried out with no lubrication, using a laboratory rolling mill with a loading capacity of 30 tons. The roll diameter was 350 mm and the rolling speed was set at 10 rpm. The literature reported the detailed procedures that were used for composite manufacturing via semi-solid stir casting [8, 34, 44, 45] and hot-rolling process [34].

For potentiodynamic polarization measurements, samples were connected to an ultra-pure copper wire and embedded in an epoxy resin holder. The surfaces were

then prepared by grinding up to 3000 grit using SiC papers followed by successively cleaning in ethanol and then distilled water using an ultrasonic bath for 15 min with each cleaning fluid. The potentiodynamic measurements were repeated three times for each sample, for each set of processing conditions, using a Princeton Applied Research, EG&G PARSTAT 2263 Advanced Electrochemical system running 2.33.0 version of the Power Suite software. The specimens embedded in epoxy resin were employed as working electrodes. A platinum rod and a saturated calomel electrode (SCE) were used as counter electrode and a reference electrode, respectively. Before measurements, samples were immersed in 3.5 wt.% NaCl solution at room temperature for 1 h, then open circuit potential (OCP) measurement was carried out for the 1800s. A scan rate of 1 mV s^{-1} was applied and the potential range studied was ±250 mV with respect to open circuit potential (OCP).

The samples were observed in a scanning electron microscope (SEM, Cam Scan MV2300, equipped with EDAX analysis) before and after the corrosion testing to determine the morphology in the regions of corrosion and corrosion effects on the materials surface.

3. Results and discussion

Figs. 1a-i show the SEM images (obtained using the backscattered electron (BSE) detector) of the rolled samples before evaluation of the corrosion test. Fig. 1a shows the SEM image of rolled A356 alloy, in which fine fragmented silicon particles were aligned along with the rolling direction. Silicon has a very low solubility in aluminium, so it precipitates as pure silicon in a coarse flake shape, which results in inhomogeneous mechanical and chemical properties. Silicon phase is cathodic with respect to the aluminium-rich matrix that could lead to the formation of micro-galvanic couples resulting in localized corrosion. However, our previous study [34] indicated that semi-solid casting process followed by intensive rolling caused severe fragmentation and refinement of eutectic silicon phase in the matrix of α-aluminium. Arrabal et al. [46] indicated that this refinement of silicon phase reduced the potential difference between secondary phases and the matrix and increased the A356 corrosion resistance.

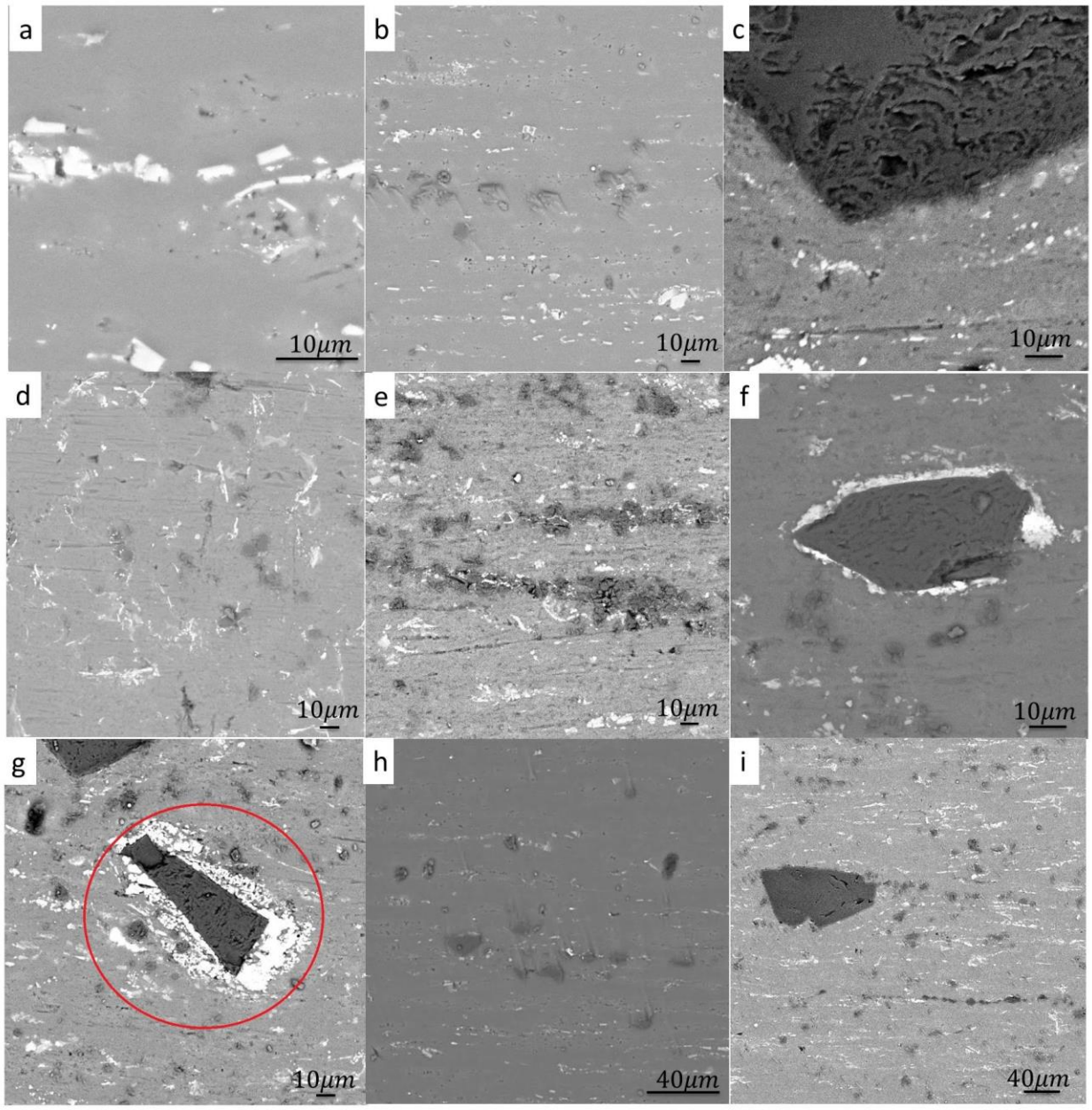

Fig. 1. SEM images of the rolled samples before corrosion test: (a) S_1, (b) S_2, (c) S_3, (d) S_4, (e) S_5, (f) S_6, (g) S_7, (h) S_8, and (i) S_9.

It has been reported in the literature [21] that the quality of nickel coating layer on the large micron-sized ceramic particles is higher than that for the fine micron-

sized particles. Therefore, the incorporation amount of fine Ni-coated SiC particles into the molten aluminium would not be considerable. This is confirmed in Fig. 1b that the incorporation of only a small amount of SiC particles was evident for sample S_2. It can be seen from Fig. 1b that these particles were aligned along with the rolling direction like the silicon particles, showing the effect of rolling process on the distribution of silicon and SiC particles. Fig. 1c shows the SEM image of sample S_3, in which a suitable interface of a large Al_2O_3 powder with with the matrix was shown, while no trace of Ni layer with a different chemical composition was observed around the particle. The separation of nickel layer from the ceramics after incorporation and stirring was also observed in other studies due to exothermic nature of reaction between nickel and molten aluminium [36, 44].

Fig. 1d shows the microstructure of sample S_4 with a distribution of SiC particles, in which just 1.5 wt. % SiC was used. In contrast with nickel, copper coating layer showed a tendency for covering the fine SiC particles with a suitable uniformity [33, 34], a higher incorporation compared with Ni-coated SiC particles [21]. Fig. 1e shows that copper coating can incorporate a higher amount of fine SiC particles for the sample S_5, and it can be observed that incorporation of higher SiC particles would lead to the higher agglomeration.

In contrast with the sample S_3 (see Fig. 1c), Fig. 1f shows the remaining of copper coating on an alumina particle for the sample S_6. Rajan et al. [36] suggested that copper layer with an endothermic nature of reaction with molten aluminium has a higher chance of remaining on the particles, and making a suitable bonding with the matrix with the formation of Al_2Cu phase. The relative atomic percents of Al and Cu elements at these areas obtained by point-EDAX analysis indicated that white-colored areas contain Al_2Cu phase. It should be noted that based on our previous studies [33, 34], observation of copper rich areas around the particles by SEM and optical microscope is depended on the thickness of the coating layer before ceramic incorporation. This remaining copper on the particles after stirring and solidification and formation of Al_2Cu phase near the matrix was also observed for the sample S_7 (see Fig. 1g), in which 1.5 wt. % of copper coated alumina and SiC particles were added to the melt. A smaller amount of agglomeration of fine SiC particles was also revealed compared to sample S_5 (Fig. 1e) mainly due to a decrease in their amount from 3 to 1.5 wt. %.

Based on our previous studies [21, 33, 34], it could be deduced that the size of ceramic particles, irrespective of their chemical composition, affects the uniformity of copper and nickel coating layers and therefore, two other samples were prepared in this study, in which various types of layers were coated on the

fine and large SiC and Al_2O_3 particles. Figs. 1h and 1i show typical SEM microstructures of the samples S_8 and S_9 (Table 4), respectively. The importance of coating type (Ni or Cu) can be clearly observed from these figures (lower magnifications used to better show this importance). In contrast with the sample S_8, an ideal distribution of alumina and in particular SiC particles was revealed for the samples S_9, in which copper coating was applied on the smaller particles and nickel layer covered the larger particles.

Fig. 2 shows the SEM morphology of A356 alloy after polarization test. It can be seen that some shallow corroded areas were formed free of the silicon phases. Many silicon phases, appearing white in these images, can be detected without any corrosion attack for the rolled alloy, showing that these attacks are not related to silicon. Fig. 3 shows the SEM morphology of sample S_2 (reinforced with 3 wt. % Ni-coated SiC particles) after corrosion test. More deep pits were detected for this sample compared with unreinforced alloy that might be caused by the presence of Al-Ni interphase compounds and fine SiC agglomeration. As mentioned [41], agglomeration of the reinforcing phases at higher concentration caused severe corrosion attack mainly via the air gap and spaces between the particles. These spaces can cause further transferring of electrons and ions, leading to the occurrence of more intensive corrosion. Table 4 showed that 2.8 g

of nickel coating layer were present around the SiC particles, while this value was 3.3 g for Al_2O_3 powders. A severe corrosion attack along with the formation of cracks and considerable number of deep pits were detected for the sample S_3 (see Fig. 4). It can be also seen that alumina particles were separated from the matrix after corrosion attack, showing that corrosion might cause the weakness of bonding. Due to the dissolution and dispersion of nickel layer in the matrix during stirring, the Al-Ni interphase compounds were dispersed in the matrix as a result of their reaction with the molten aluminium. It is reported that Al-Ni intermetallic phases have different potentials from that matrix alloy [47], therefore a localized galvanic cell may be formed between these phases and the matrix. These phases are cathodic to the Al matrix and decrease the corrosion resistance in NaCl media. In contrast, it is reported that the presences of SiC and Al_2O_3 does not lead to the galvanic corrosion in the Al-SiC and Al-Al_2O_3 composites at the matrix/particle interface [48-50]. Galvanic corrosion between Al_2O_3 phase and aluminium is unlikely, because resistivity of Al_2O_3 is greater than 1000 Ωcm. The Al_2O_3/aluminium AMMCs possesses excellent corrosion resistance due to a lack of galvanic action with the Al_2O_3 phase [50]**.** Therefore, the reason of corrosive attack for such materials is not due to the presence of this ceramic. Unsuitable interfaces between the metal and ceramic, agglomeration of ceramics, and the

electrochemical interactions between the metallic coating layer and the aluminium matrix might be detrimental for corrosion resistance of such materials.

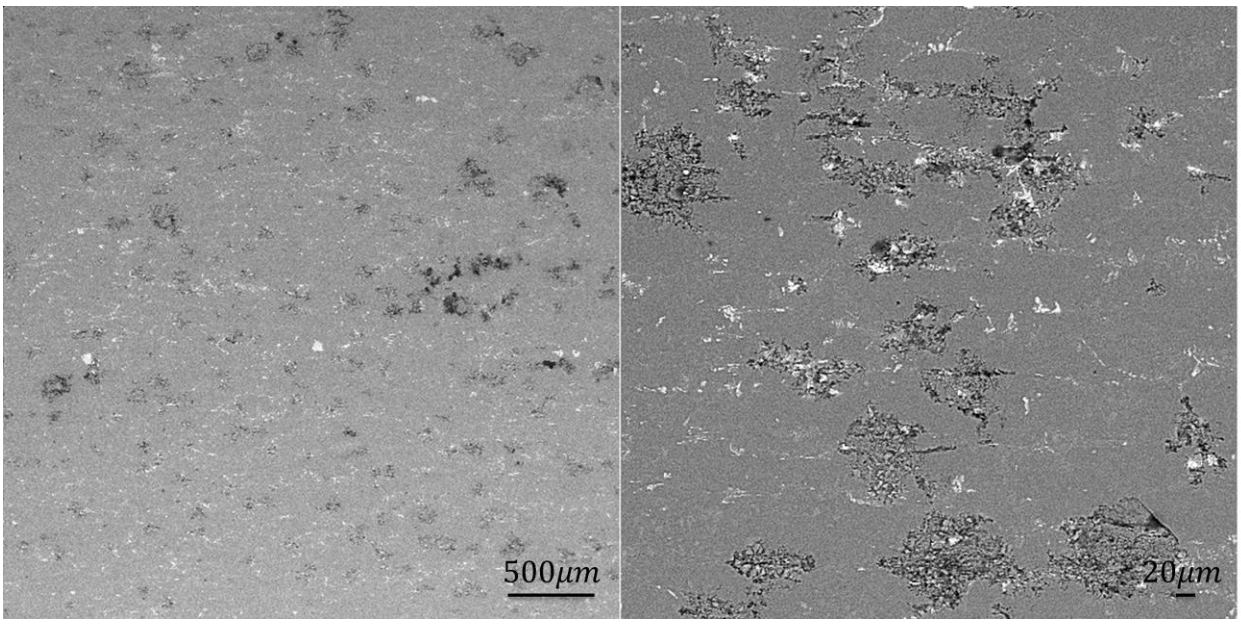

Fig. 2. SEM image of the rolled sample S_1 after corrosion test.

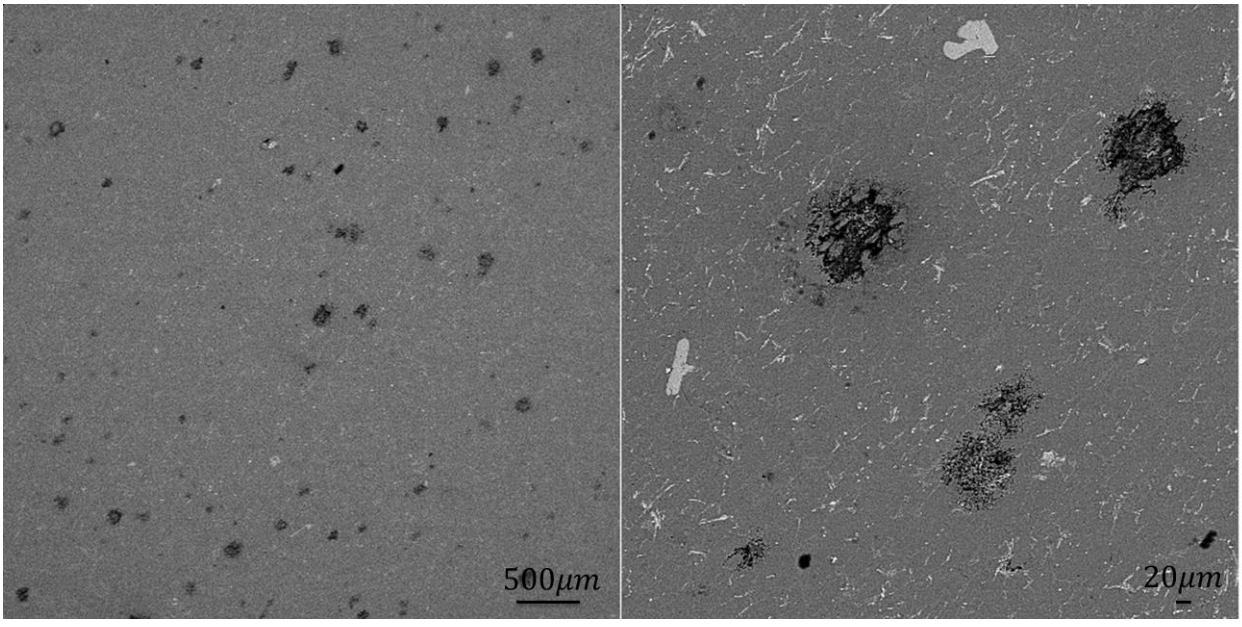

Fig. 3. SEM image of the rolled sample S_2 after corrosion test.

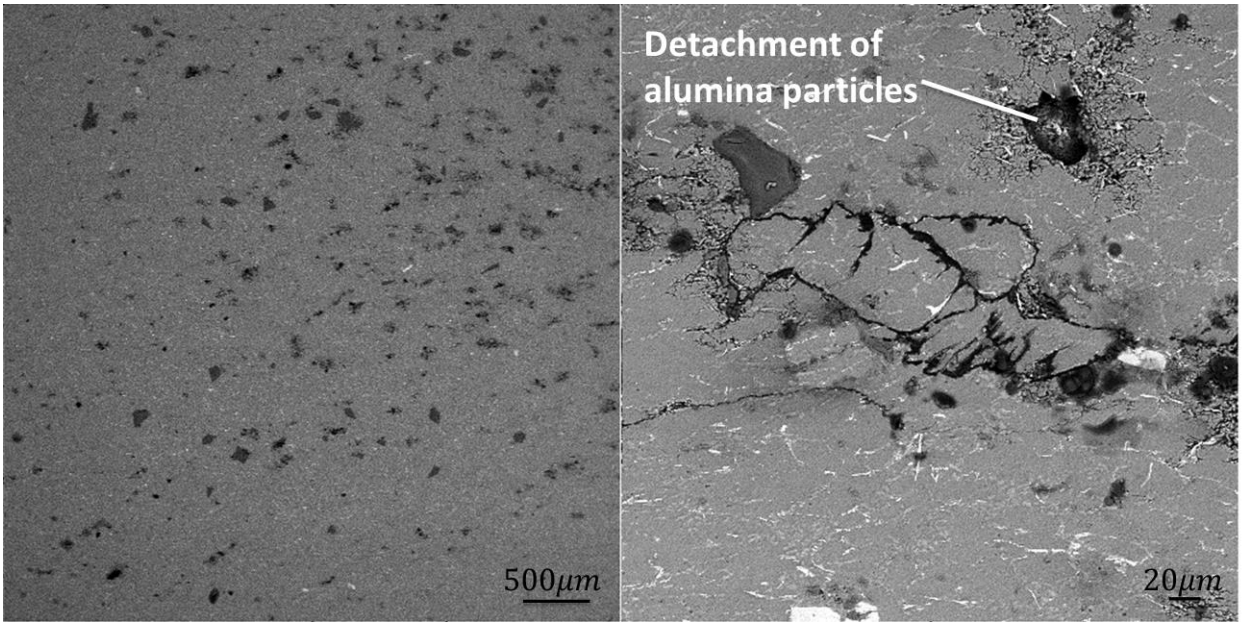

Fig. 4. SEM image of the rolled sample S_3 after corrosion test.

Figs. 5a and b show the SEM/EDAX analysis for the sample S_4 reinforced with Ni-coated hybrid ceramic particles. Although, the number of attacked areas is not as much as the previous sample S_3, detachment of alumina and SiC particles could be seen in Figs. 5 (a) and (b) respectively. The lower number of corrosion pits for the sample S_4 (with a lower value of nickel weight than that of sample S_3, see Table 4) with respect to that of sample S_3 indicated that the incorporation of nickel into the molten aluminium and formation of Al-Ni binary compounds might reduce the corrosion resistance. EDAX analysis (point A, Fig. 5b) indicated the presence of oxygen and chlorine elements at the interface of detached SiC particles with the aluminium matrix. Osorio et al. [48] indicated that a eutectic mixture of Al_3Ni intermetallic phase with the aluminium matrix acts as a cathodic area in a matrix

of aluminium in NaCl solution. They schematically showed that the presence of Al-Ni binary compounds reduced the corrosion resistance of aluminium and their presence aids the chlorine ions for the attack to the aluminium matrix. Figs. 6 and 7 show the suggested mechanism for the corrosion attack in the samples contain Ni-coated Al_2O_3 and SiC particles, respectively. This mechanism was drawn from the SEM/EDAX results shown in Figs. (3-5). It can be seen from Figs. 6 and 7 that geometrically necessary dislocations (GNDs) were formed after solidification around the ceramic particles with a different coefficient of thermal expansion than that of the aluminium matrix. Therefore, high-energy areas were formed around the the particles that are susceptible to the corrosion. The separation of nickel coating layer from the particles and its dissolution and interaction with the molten aluminium caused the formation of Al-Ni binary compounds that are cathodic with respect to the aluminium matrix [48]. Therefore, microgalvanic couples were formed in the areas containing the nickel phase, leading to the transfer of electrons, which could affect the high-energy areas around the ceramic particles by promoting corrosive attack. On the other hand, a reaction between the alumina surface layer with chlorine ions [51] destroys this protecting layer by formation of $AlCl_3$ and oxygen, resulting in a further entrance of chlorine ions into the matrix and around the ceramic particles. EDAX analysis in Fig. 5b

shows the presence of nickel rich areas around the ceramic particles (point B) and detection Cl and O elements at the interface of SiC/Al. $AlCl_3$ will react with water to form aluminium hydroxide and HCl, leading to a reduction in pH of the water around the surface. A new alumina surface layer will be formed by the dissociation of $Al(OH)_3$ into the Al_2O_3 and water. These occurrences led to the detachment of some of the ceramic particles and Al_3Ni intermetallic compounds from the matrix by losing the coating bonding.

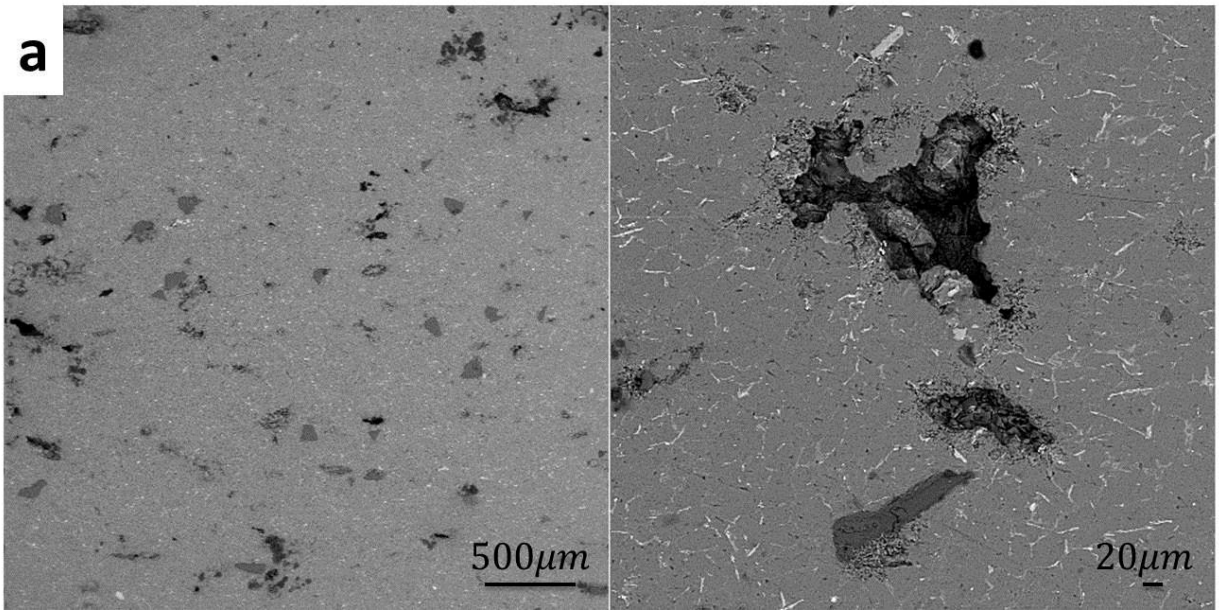

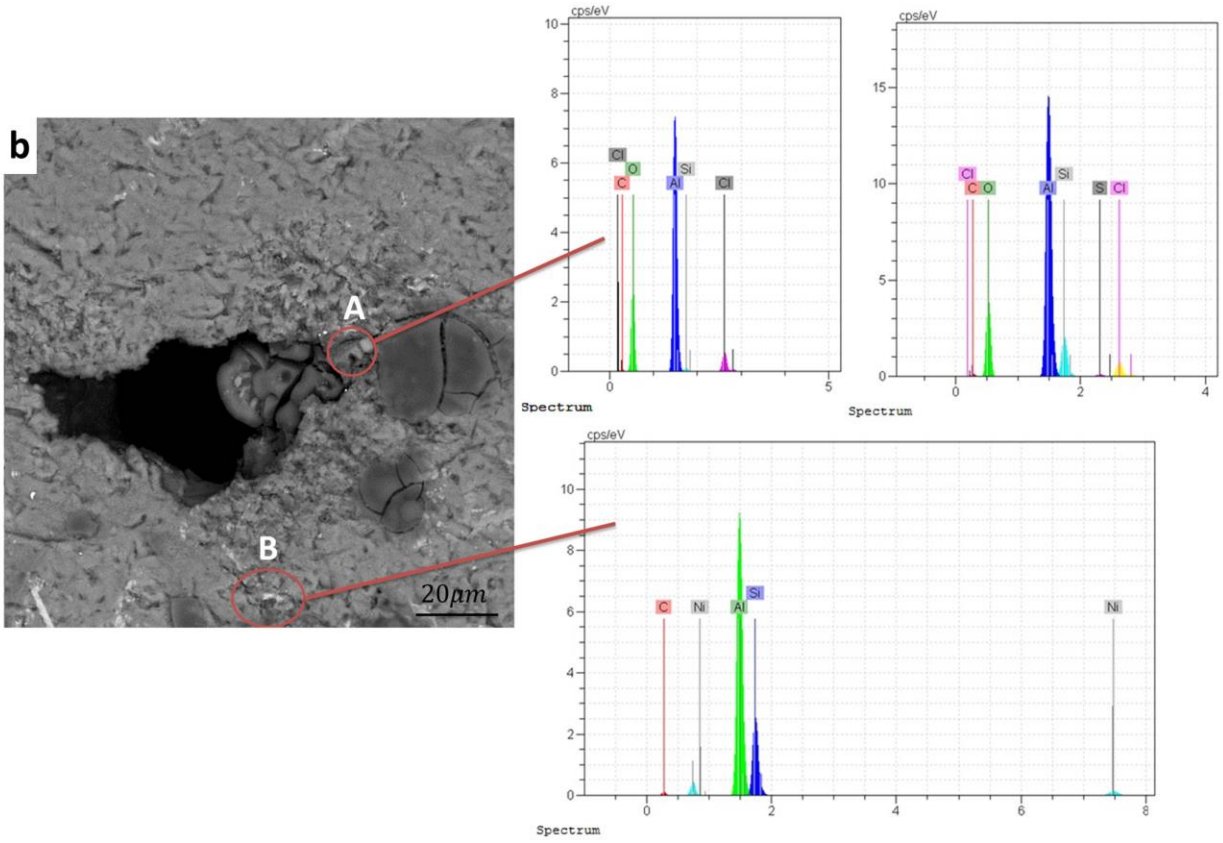

Fig. 5. SEM image of the rolled sample S_4 after corrosion test (a), EDAX analysis of marked points A and B (b).

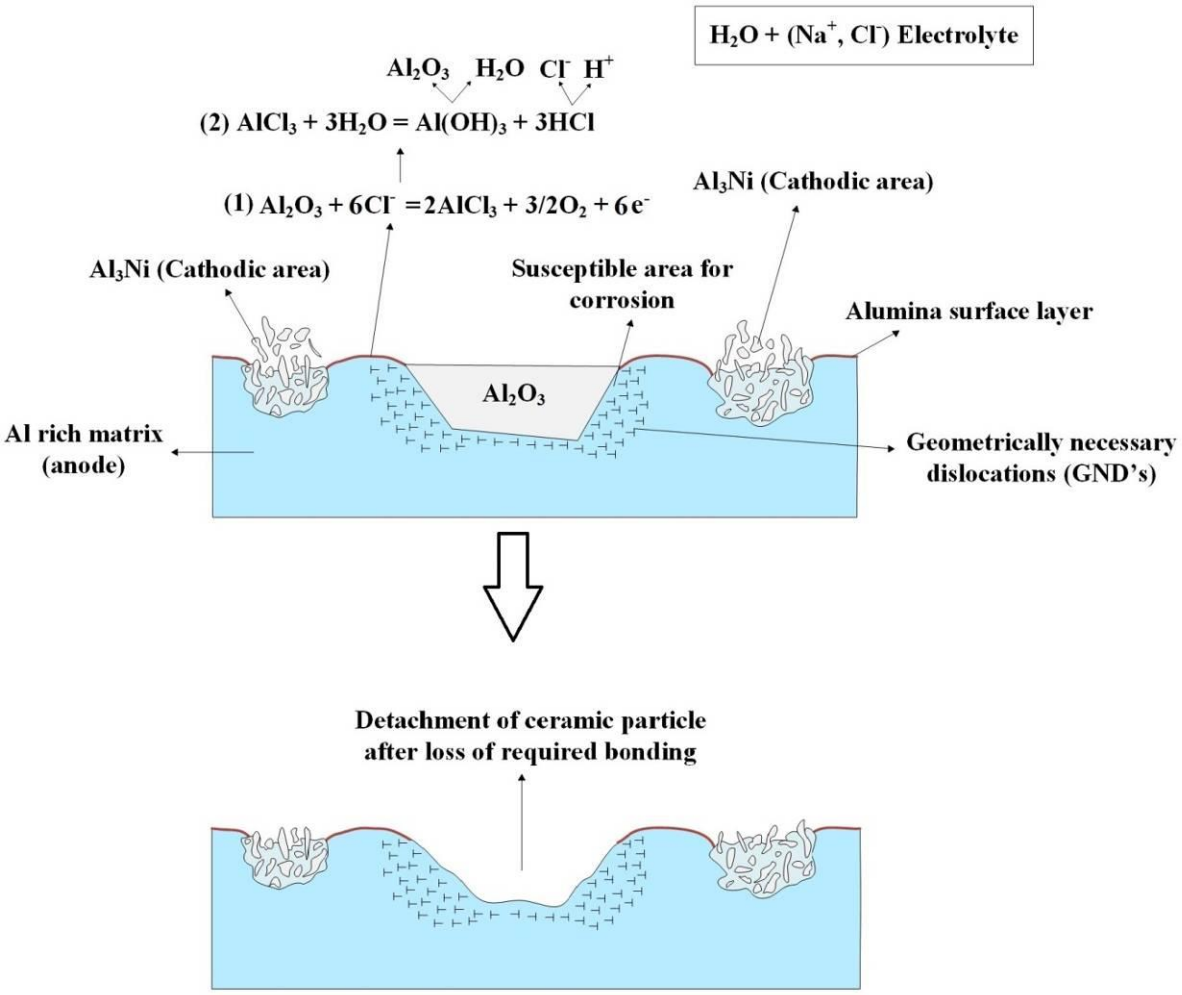

Fig. 6. The schematic of suggested mechanism for corrosion attack in areas contain Ni-coated Al_2O_3 particles.

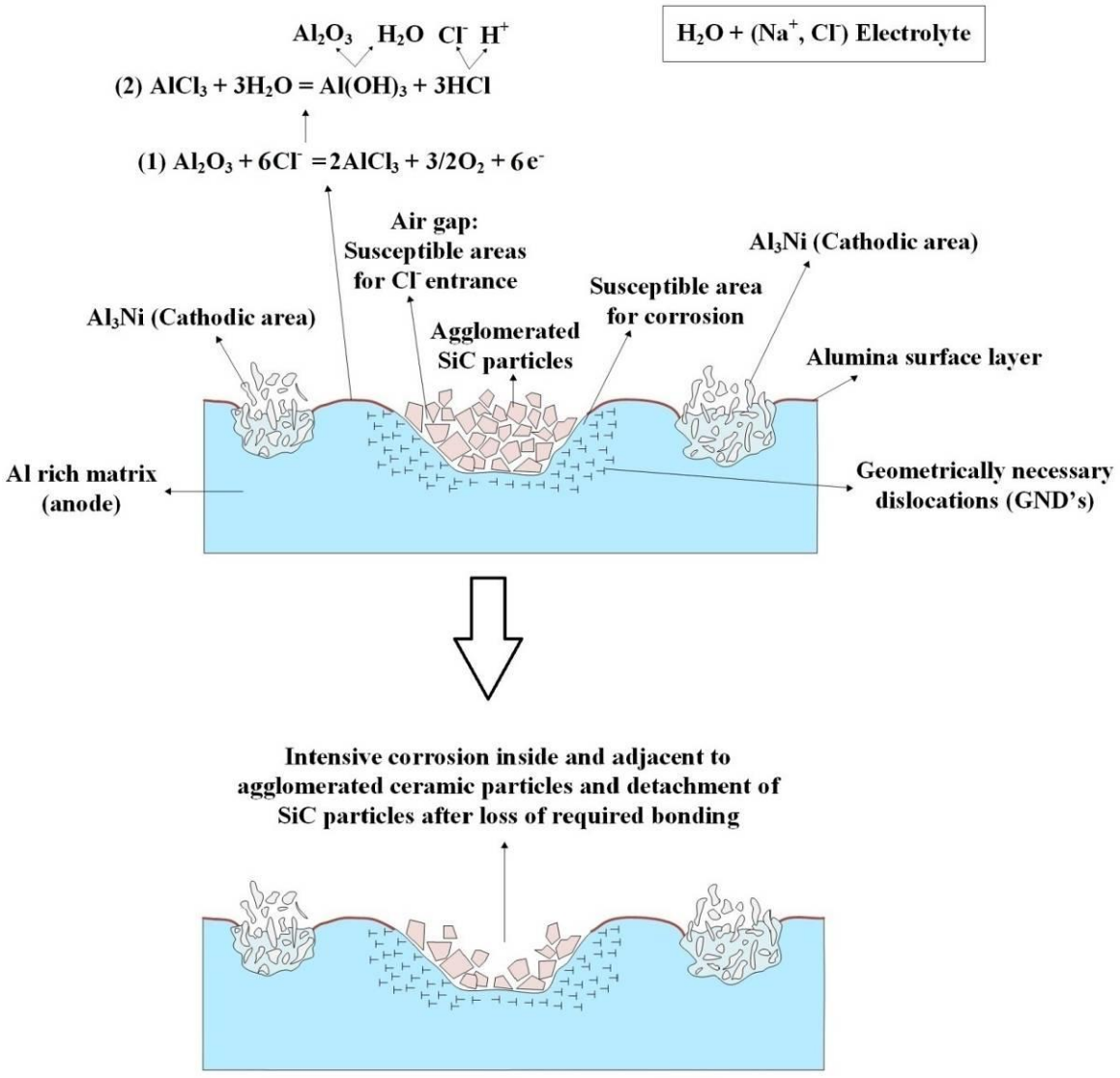

Fig. 7. The schematic of suggested mechanism for corrosion attack in areas contain Ni-coated SiC particles.

In contrast with Al-Ni binary compounds, literature [52, 53] reported that Al_2Cu phase is not active in the matrix of aluminium. Such noble interphase compounds in the aluminium matrix could not make microgalvanic couples and affect the

corrosion resistance. Figs. (8-10) show the SEM images of samples $S_{(5-7)}$, respectively. In can be seen that the number of pits is considerable for the sample S_5 reinforced by fine Cu-coated SiC particles with respect to the samples S_6 and S_7, in which lower ceramic agglomeration occurred. However, by comparing Figs. (3-5) with Figs. (8-10), it was found that the number of corrosion pits for the samples reinforced by Cu-coated particles is less than that of the samples reinforced by Ni-coated particles. It seems that corrosion attack was not considerable, in particular for the sample S_6 reinforced by Cu-coated alumina particles, indicating that microgalvanic couple between the metallic coating layer and the matrix as well as ceramic agglomeration are the two main reasons for corrosion occurrence in such materials.

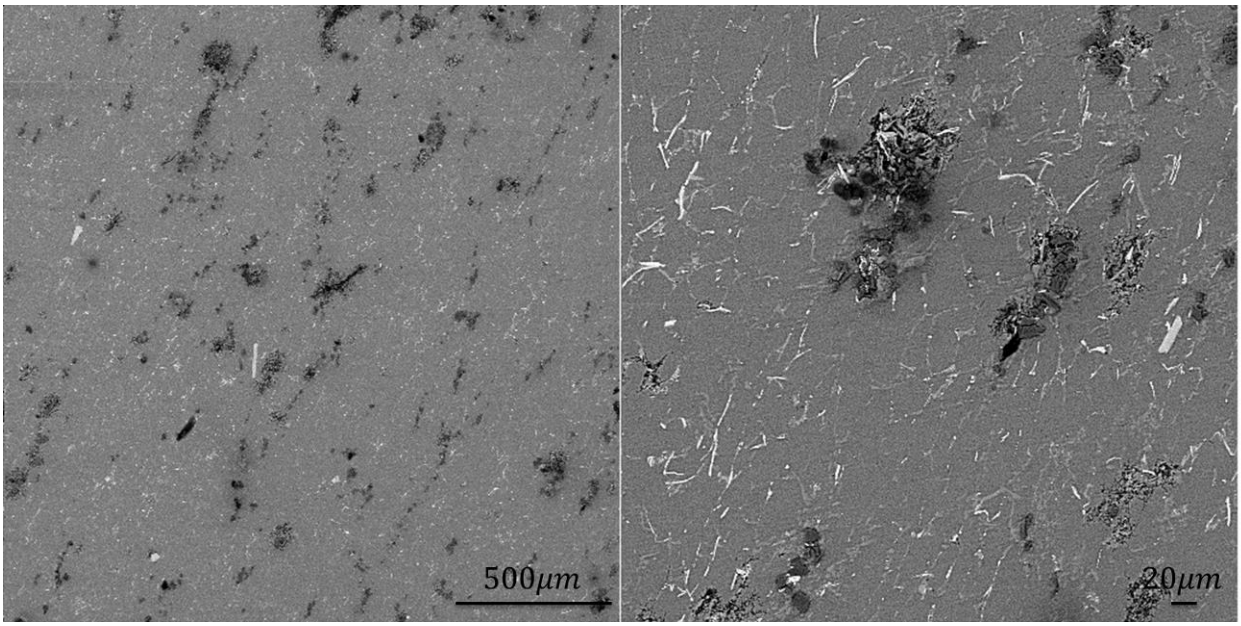

Fig. 8. SEM image of the rolled sample S_5 after corrosion test.

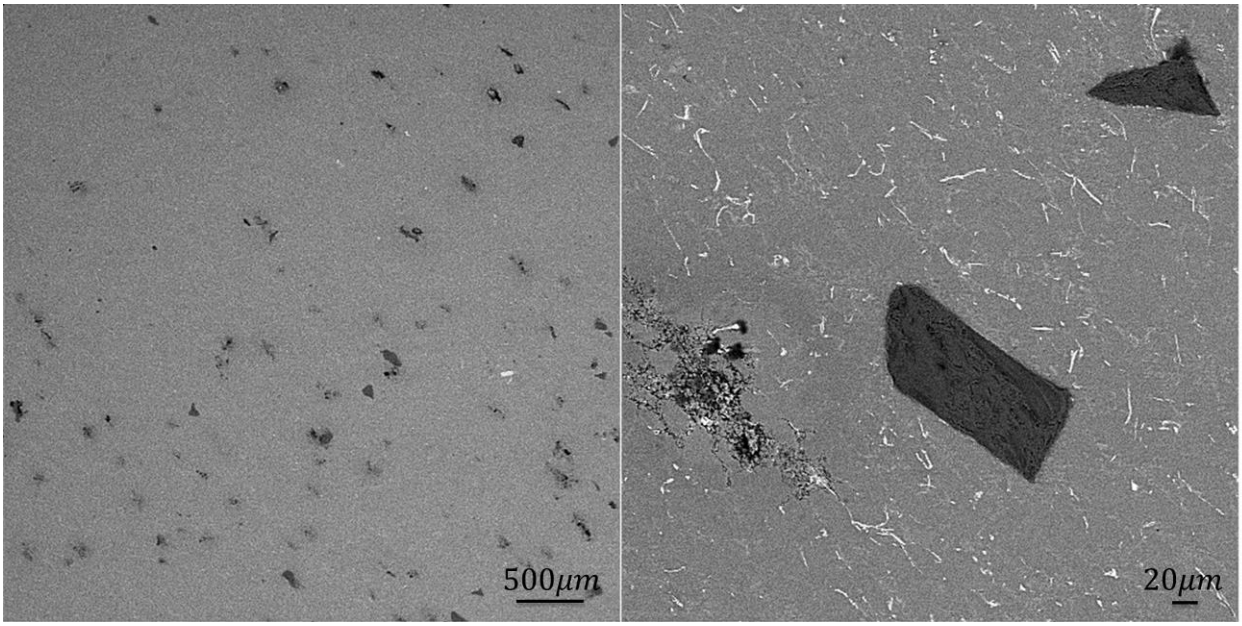

Fig. 9. SEM image of the rolled sample S_6 after corrosion test.

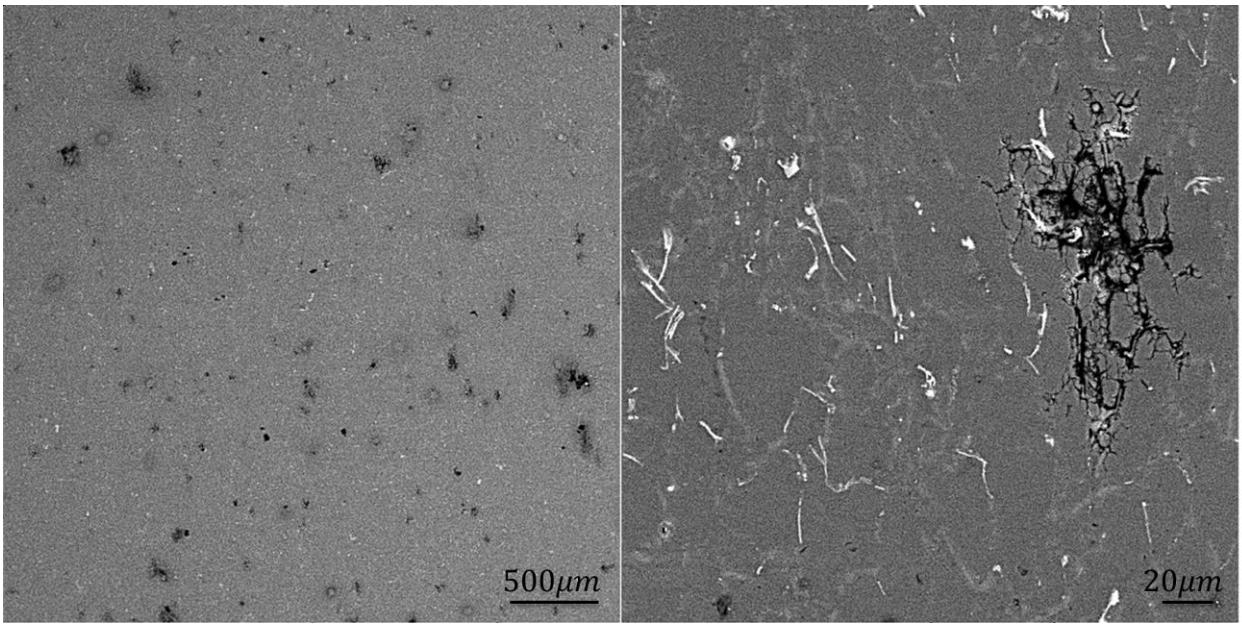

Fig. 10. SEM image of the rolled sample S_7 after corrosion test.

As mentioned, two other samples reinforced by ceramics with bimodal coated particles were prepared to further understand the effect of nickel and copper coating layers on the corrosion occurrence. Figs. 11 and 12 show the SEM images

for the samples S_8 and S_9, respectively, after corrosion analysis. Deep pits as well as detachment of ceramic particles were again revealed for these samples possibly due to the presence of nickel in the matrix. However, by consideration of Figs. 3-5 with Figs. 11 and 12, it can be found that more severe corrosion attack seems to occur for the samples $S_{(2\text{-}4)}$, in which just nickel coating layer was applied to the ceramics.

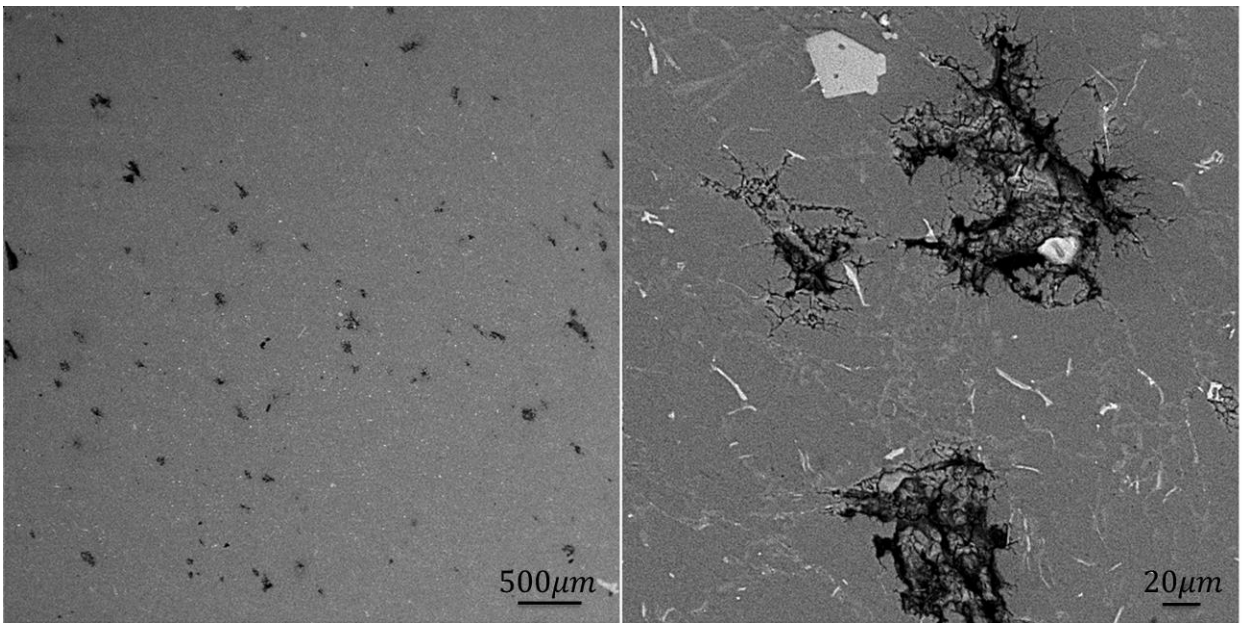

Fig. 11. SEM image of the rolled sample S_8 after corrosion test.

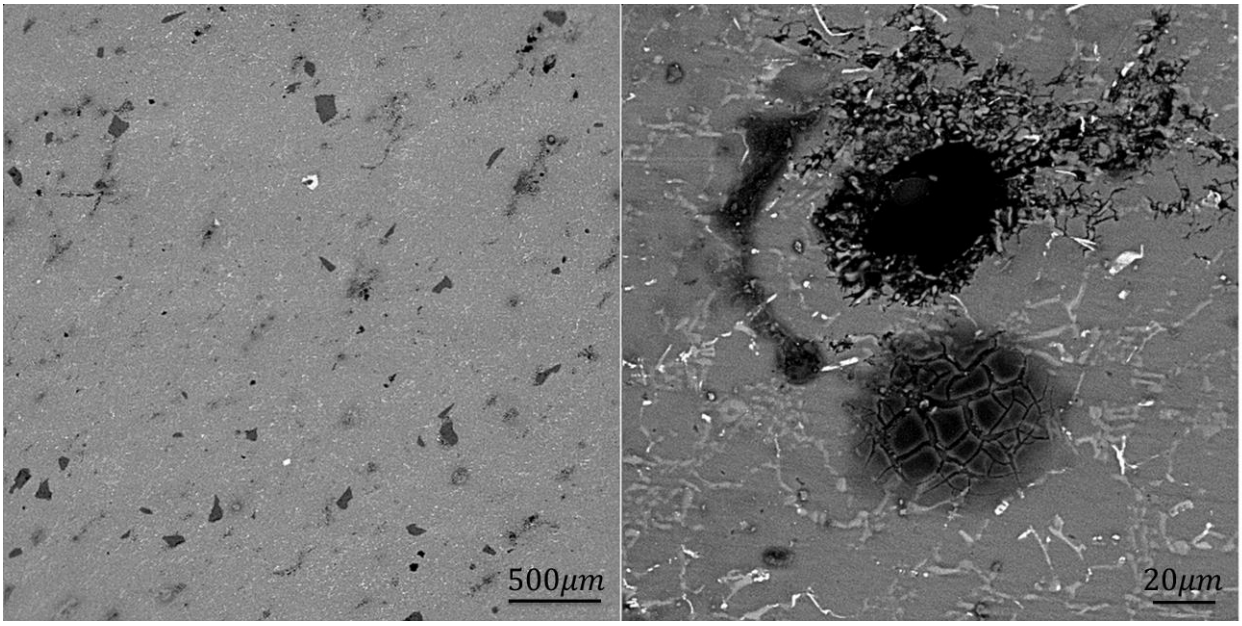

Fig. 12. SEM image of the rolled sample S_9 after corrosion test.

Fig. 13 shows the variations in OCP of samples S_1 to S_9 in the 3.5 wt.% NaCl aqueous solution. According to this figure, it can be seen that all of the samples were completely stable after 1800 s, and also the composite samples showed to have a lower potential than Sample S_1, which can be related to the presence of ceramic and intermetallic particles and occurrence of microgalvanic corrosion between them and the matrix.

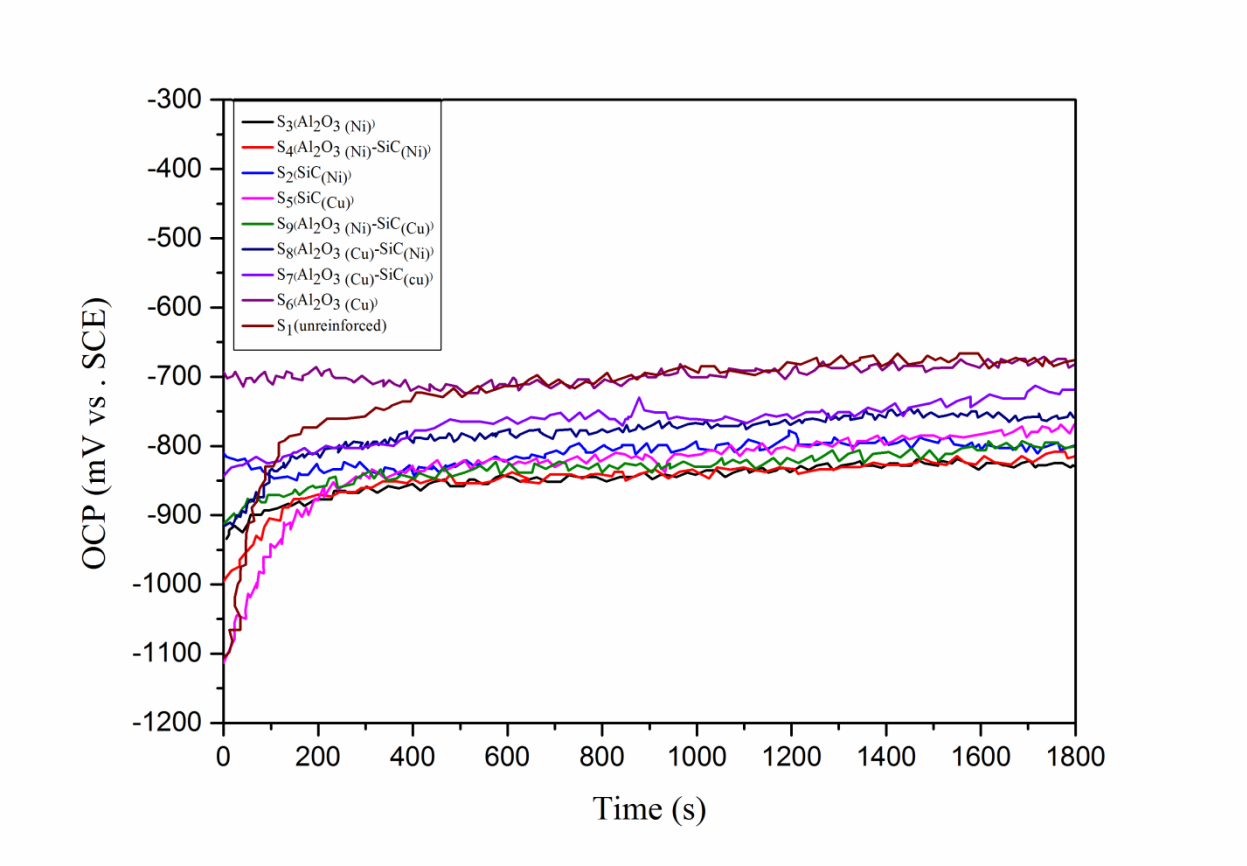

Fig. 13. OCP–time measurement curves for the samples.

Potentiodynamic polarization measurements for the samples are required for obtaining the behaviour and response of the samples against a specified range of potential in 3.5 wt.% NaCl aqueous solution. Fig. 14 shows the results of a typical Tafel polarization measurement for the samples, and Table 5 tabulated the detailed results of polarization test. By a comparison between Tables 4 and 5, it can be seen that there is a direct relationship between the weight of incorporated nickel and corrosion current density, in which a higher nickel presence in the matrix caused an increase in the corrosion current density. However, it can be

observed that sample S_5, which contained fine Cu-coated SiC particles, did not follow this rule. Fig. 1e shows the considerable agglomeration of fine SiC particles for this sample. Such sites have the potential for the corrosion attack and transfer of electrons. The adherence of alumina oxide layer is not high enough in such areas. It can be seen that this sample showed poor corrosion resistance. In sample S_6, in which the copper coating was used and no agglomeration of the ceramic particles occurred, almost similar corrosion behaviour to the A356 aluminium alloy was observed.

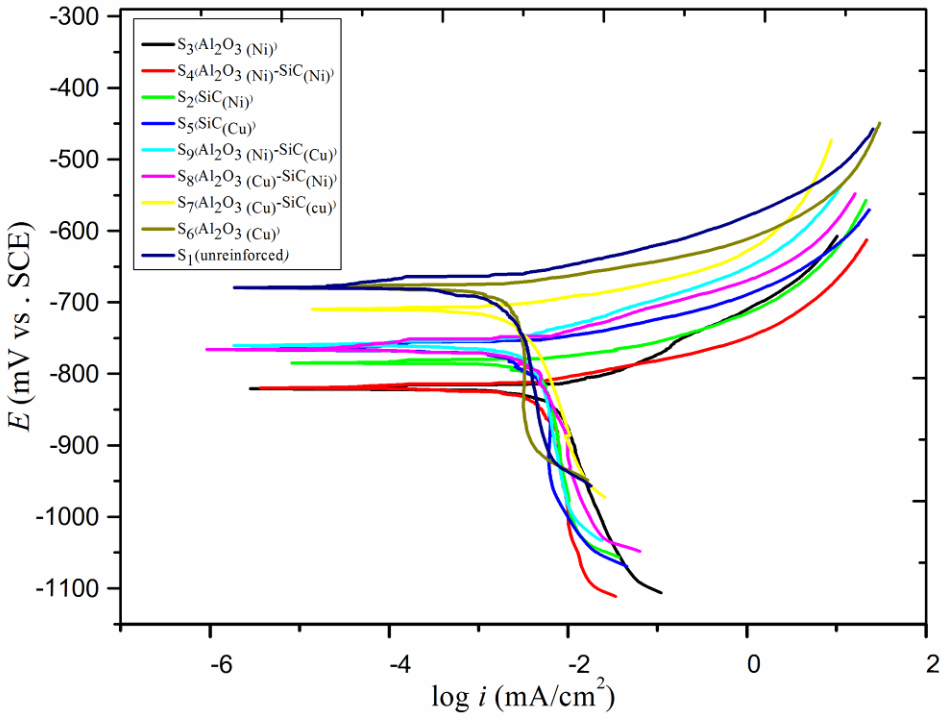

Fig. 14. Typical Tafel polarization curves for the samples in 3.5 wt% NaCl at 25℃.

Table 5

Results of Tafel polarization in 3.5 wt% NaCl at 25℃.

Samples	E_{Corr}(mV)	I_{corr}(μA cm^{-2})	β_a(mV dec^{-1})	$-\beta_c$(mV dec^{-1})
$S_{3\ (Al_2O_{3_{Ni}})}$	-830.30	8.21	55.41	351.07
$S_{4\ (Al_2O_{3_{Ni}}-SiC_{Ni})}$	-818.81	6.10	33.85	562.32
$S_{2\ (SiC_{Ni})}$	-799.39	5.90	33.02	542.84
$S_{5\ (SiC_{Cu})}$	-770.44	4.9	34.53	726.27
$S_{9\ (Al_2O_{3_{Ni}}-SiC_{Cu})}$	-750.86	4.5	37.15	633.38
$S_{8\ (Al_2O_{3_{Cu}}-SiC_{Ni})}$	-757.54	4.25	36.74	420.45
$S_{7\ (Al_2O_{3_{Cu}}-SiC_{Cu})}$	-718.22	3.39	37.97	540.21
$S_{6\ (Al_2O_{3_{Cu}})}$	-680.91	2.80	30.32	326.22
$S_{1\ (unreinforced)}$	-675.10	2.70	37.94	540.21

It can be seen that there is a good agreement between the potential and current density of corrosion for the samples, showing that most of the samples with a higher corrosion current density have a more negative potential.

4. Conclusion

In this study, the potentiodynamic polarization curves were obtained from the rolled unreinforced and reinforced A356 aluminium alloy to determine the main effective factors on the corrosion resistant of the materials. From the experimental results, the followings could be drawn:

1. Various types of hybrid ceramic reinforced composites with elongated reinforcing particles were prepared with a suitable distribution after semi-solid casting followed by a hot-rolling process.

2. The copper coating layer showed a higher tendency for remaining around ceramic particles after solidification and rolling processes.

3. SEM analysis of the samples after corrosion test indicated the presence of shallow corroded areas on the matrix of A356 unreinforced alloy, while deeper corroded areas were observed around the large-sized Ni-coated Al_2O_3 particles.

4. SEM analysis indicated that fine SiC agglomeration caused serious corrosion attack for both the composites reinforced by Cu and Ni coated particles. In addition, it was found that by increasing the amount of Ni, a higher corrosion attack occurred in the matrix.

5. Based on the polarization test results, a higher amount of incorporated nickel transmitted by the large-sized Al_2O_3 led to the lowest corrosion resistance among all of the samples.

6. In contrast with nickel, no significant stimulation of Al-Cu compounds on corrosion of the matrix was observed and it was found that Cu-coated Al_2O_3 composite had the best corrosion resistance, after that of the unreinforced alloy.

References

[1] S. Prasad, R. Asthana: Tribol. Lett. 17 (2004) 445. DOI: 10.1023/B:TRIL.0000044492.91991.f3
[2] M. Mohammadpour, R.A. Khosroshahi, R.T. Mousavian, D. Brabazon: Ceram. Int. 40 (2014) 8323. DOI: 10.1016/j.ceramint.2014.01.038
[3] Y.-M. Han, X. Chen: Materials, 8 (2015) 6455. DOI: 10.3390/ma8095314
[4] S. Vijayarangan, N. Rajamanickam, V. Sivananth: Mater.Des. 43 (2013) 532. DOI: 10.1016/j.matdes.2012.07.007
[5] M. Roshan, T.R. Mousavian, H. Ebrahimkhani, A. Mosleh: J. Min. Metal. Sect. B. 49 (2013) 299. DOI: 10.2298/JMMB120701032R
[6] A. Pardo, M. Merino, S. Merino, F. Viejo, M. Carboneras, R. Arrabal: Corros. Sci. 47 (2005) 1750. DOI: 10.1016/j.corsci.2004.08.010
[7] E. Karakulak, R. Yamanoğlu, U. Erten, A. Zeren, S. Zor, M. Zeren: Mater. Des. 59 (2014) 33. DOI: 10.1016/j.matdes.2014.02.039
[8] N. Valibeygloo, R.A. Khosroshahi, R.T. Mousavian: Int. J. Met. Mater. 20 (2013) 978. DOI: 10.1007/s12613-013-0824-2
[9] M. Mohammadpour, R.A. Khosroshahi, R.T. Mousavian, D. Brabazon: Metall. Mater. Trans. B. 46 (2015) 12. DOI:10.1007/s11663-014-0186-9
[10] H. Ye: J. Mater.Eng. Perfotm. 12 (2003) 288. DOI: 10.1361/105994903770343132
[11] T.S. Srivatsan, T. Sudarshan, E. Lavernia: Prog. Mater Sci. 39 (1995) 317. DOI: 10.1016/0079-6425(95)00003-8
[12]A.F. Boostani, S. Tahamtan, S. Yazdani, R.A. Khosroshahi, D. Wei, H. Sahamirad, X. Zhang, Z. Jiang: Scr. Mater. 118 (2016) 65. DOI: 10.1016/j.scriptamat.2016.02.028
[13] A.F. Boostani, S. Tahamtan, Z. Jiang, D. Wei, S. Yazdani, R.A. Khosroshahi, R.T. Mousavian, J. Xu, X. Zhang, D. Gong: Compos. Part A. Appl S. 68 (2015) 155. DOI:10.1016/j.compositesa.2014.10.010
[14] R. Kheirifard, N.B. Khosroshahi, R.A. Khosroshahi, R.T. Mousavian, D. Brabazon: J. Mat. Des. Appli. (2016) 1464420716649631. DOI:10.1177/1464420716649631
[15] R.T. Mousavian, R.A. Khosroshahi, S. Yazdani, D. Brabazon, A. Boostani: Mater. Des. 89 (2016) 58. DOI: 10.1016/j.matdes.2015.09.130
[16] A.F. Boostani, R.T. Mousavian, S. Tahamtan, S. Yazdani, R.A. Khosroshahi, D. Wei, J.Z. Xu, D. Gong, X. Zhang, Z. Jiang: Mat. Sci. Eng A. 648 (2015) 92. DOI: 10.1016/j.msea.2015.09.050
[17] R.T. Mousavian, R.A. Khosroshahi, S. Yazdani, D. Brabazon: Rare. Met. (2016) 1. DOI:10.1007/s12598-015-0689-9
[18] A.F. Boostani, R.T. Mousavian, S. Tahamtan, S. Yazdani, R.A. Khosroshahi, D. Wei, J. Xu, X. Zhang, Z. Jiang:Mat. Sci. Eng A. 653 (2016) 99. DOI:10.1016/j.msea.2015.12.008
[19] A.F. Boostani, S. Yazdani, R.T. Mousavian, S. Tahamtan, R.A. Khosroshahi, D. Wei, D. Brabazon, J. Xu, X. Zhang, Z. Jiang: Mater. Des. 88 (2015) 983. DOI: 10.1016/j.matdes.2015.09.063
[20] S. Naher, D. Brabazon, L. Looney: J. Mater. Process. Technol. 166 (2005) 430. DOI: 10.1016/j.jmatprotec.2004.09.043
[21] N.B. Khosroshahi, R.A. Khosroshahi, R.T. Mousavian, D. Brabazon: Ceram. Int. 40 (2014) 12149. DOI: 10.1016/j.ceramint.2014.04.055
[22] J. Hashim, L. Looney, M. Hashmi: J. Mater. Process. Technol. 119 (2001) 329. DOI: 10.1016/S0924-0136(01)00919-0
[23] S. Naher, D. Brabazon, L. Looney: J. Mater. Process. Technol. 143 (2003) 567.DOI: 10.1016/S0924-0136(03)00368-6
[24] O. Lashkari, R. Ghomashchi: J. Mater. Process. Technol. 182 (2007) 229. DOI: 10.1016/j.jmatprotec.2006.08.003

[25] I. El-Mahallawi, Y. Shash, K. Eigenfeld, T. Mahmoud, R. Ragaie, A. Shash, M. El Saeed: Mater. Sci. Technol. 26 (2010) 1226. DOI: 10.1179/174328409X441229
[26] D. Brabazon, D. Browne, A. Carr:Mat. Sci. Eng A. 326 (2002) 370. DOI: 10.1016/S0921-5093(01)01832-9
[27] J. Hashim, L. Looney, M. Hashmi: J. Mater. Process. Technol. 92 (1999) 1. DOI: 10.1016/S0924-0136(99)00118-1
[28] C. Quaak, M. Horsten, W. Kool:Mat. Sci. Eng A. 183 (1994) 247. DOI: 10.1016/0921-5093(94)90909-1
[29] M. Paes, E. Zoqui: Mat. Sci. Eng A. 406 (2005) 63. DOI: 10.1016/j.msea.2005.07.018
[30] D. Kirkwood: Int. Mater. Rev. 39 (1994) 173.DOI: 10.1179/imr.1994.39.5.173
[31] P. Seo, C. Kang, S. Lee: Int. J. Adv. Manuf. Tech. 43 (2009) 482-499. DOI: 10.1007/s00170-008-1730-z
[32] H. Noori, R.T. Mousavian, R.A. Khosroshahi, D. Brabazon, S. Damadi: Surf. Eng. 32 (2016) 391. DOI: 10.1179/1743294415Y.0000000035
[33] N. Beigi Khosroshahi, R. Azari Khosroshahi, R. Taherzadeh Mousavian, D. Brabazon: Surf. Eng. 30 (2014) 747. DOI: 10.1179/1743294414Y.0000000335
[34] N.B. Khosroshahi, R.T. Mousavian, R.A. Khosroshahi, D. Brabazon: Mater. Des. 83 (2015) 678. DOI: 10.1016/j.matdes.2015.06.027
[35] P. Rohatgi: J. Mater. Sci. 16 (1981) 1599. DOI: 10.1007/BF02396877
[36] T. Rajan, R. Pillai, B. Pai: J. Mater. Sci. 33 (1998) 3491. DOI: 10.1023/A:1004674822751
[37] A.S. Verma, N.M. Suri: Mater. Today.Proc. 2 (2015) 2840. DOI: 10.1016/j.matpr.2015.07.299
[38] B. Wielage, A. Dorner: Compos. Sci. Technol.59 (1999) 1239. DOI: 10.1016/S0266-3538(98)00163-8
[39] A. Pardo, M. Merino, R. Arrabal, S. Merino, F. Viejo, A. Coy: Surf. Coat.Technol. (2006). DOI:10.1016/j.surfcoat.2005.05.028
[40] E. Marin, M. Lekka, F. Andreatta, L. Fedrizzi, G. Itskos, A. Moutsatsou, N. Koukouzas, N. Kouloumbi: Mater. Charact. 69 (2012) 16. DOI: 10.1016/j.matchar.2012.04.004
[41] I. Singh, D. Mandal, M. Singh, S. Das: Corros. Sci. 51 (2009) 234. DOI: 10.1016/j.corsci.2008.11.001
[42] G. Kiourtsidis, S.M. Skolianos: Mat. Sci. Eng A. 248 (1998) 165. DOI: 10.1016/S0921-5093(98)00494-8
[43] M.A. El-Khair, A.A. Aal: Mat. Sci. Eng A. 454 (2007) 156. DOI: 10.1016/j.msea.2006.11.145
[44] R.T. Mousavian, S. Damadi, R.A. Khosroshahi, D. Brabazon, M. Mohammadpour: Int. J. Adv. Manuf. Tech. 81 (2015) 433. DOI: 10.1007/s00170-015-7246-4
[45] S. Soltani, R.A. Khosroshahi, R.T. Mousavian, Z.-Y. Jiang, A.F. Boostani, D. Brabazon: Rare .Met. (2015) 1. DOI:10.1007/s12598-015-0565-7
[46] R. Arrabal, B. Mingo, A. Pardo, M. Mohedano, E. Matykina, I. Rodríguez: Corros. Sci. 73 (2013) 342. DOI:10.1016/j.corsci.2013.04.023
[47] B. Dikici, C. Tekmen, M. Gavgali, U. Cocen: J. Mech.Eng. 57(2011) 11. DOI:10.5545/sv-jme.2010.111
[48] W.R. Osorio, E.S. Freitas, J.E. Spinelli, M.V. Cante, C.R. Afonso, A. Garcia: Int. J. Electrochem. Sci, 7 (2012) 9946.
[49] E. Darmiani, I. Danaee, M. Golozar, M. Toroghinejad: J. Alloys Compd. 552 (2013) 31-39. DOI: 10.1016/j.jallcom.2012.10.069
[50] B. Bobić, S. Mitrović, M. Babić, I. Bobić:Tribology in industry. 32 (2010).
[51] R.T. Mousavian, E. Hajjari, D. Ghasemi, M.K. Manesh, K. Ranjbar:Eng. Fail. Anal. 18 (2011) 202. DOI: 10.1016/j.engfailanal.2010.08.022
[52] K.S. Rao, K.P. Rao: Trans. Indian Ins. Met. 57 (2004) 593.
[53] R.P. Wei, C.-M. Liao, M. Gao: Metall. Mater. Trans. A. 29 (1998) 1153. DOI: 10.1007/s11661-998-0241-8